

# Lepton Flavour Violation in the Constrained MSSM with Natural Neutrino Mass Hierarchy

T. Blažek\* and S. F. King

*Department of Physics and Astronomy, University of Southampton  
Southampton, SO17 1BJ, U.K*

## Abstract

We present predictions for  $\mu \rightarrow e\gamma$  and  $\tau \rightarrow \mu\gamma$  in the CMSSM in which there is a natural hierarchy of neutrino masses resulting from the sequential dominance of three right-handed neutrinos. We perform a global analysis of this model in the  $(m_0, M_{1/2})$  plane, assuming radiative electroweak symmetry breaking, and including all observed laboratory data. We confirm that a large (small)  $\tau \rightarrow \mu\gamma$  rate results from the dominant right-handed neutrino being the heaviest (lightest) one. We show that the  $\mu \rightarrow e\gamma$  rate may determine the order of the sub-dominant neutrino Yukawa couplings in the flavour basis, but may also be sensitive to effects beyond the leading log and leading mass insertion approximations. We also show that the  $\mu \rightarrow e\gamma$  rate is independent of  $\theta_{13}$ , but measurement of this angle may determine a ratio of sub-dominant Yukawa couplings.

October 31, 2018

\*On leave of absence from the Dept. of Theoretical Physics, Comenius Univ., Bratislava, Slovakia

# 1 Introduction

Atmospheric and solar neutrino experiments have provided convincing evidence for neutrino masses and mixings. The current minimal best fit interpretation of the data involves three light neutrinos with [1]

$$|\Delta m_{32}^2| = (1.7 - 3.3)10^{-3}\text{eV}^2, \quad \sin^2 2\theta_{23} = 0.93 - 1.0, \quad (1)$$

$$\Delta m_{21}^2 = (4 - 10)10^{-5}\text{eV}^2, \quad \sin^2 2\theta_{12} = 0.71 - 0.89, \quad (2)$$

where  $m_{ij}^2 = m_i^2 - m_j^2$  are the neutrino mass squared differences and the approximate  $1\sigma$  ranges are shown. These masses and mixings represent the first solid evidence of new physics beyond the Standard Model.

The most elegant explanation of small neutrino masses continues to be the see-saw mechanism [2, 3]. According to the see-saw mechanism, lepton number is broken at high energies due to right-handed neutrino Majorana masses, resulting in small left-handed neutrino Majorana masses suppressed by the heavy mass scale. A natural implementation of the see-saw mechanism which can account for a neutrino mass hierarchy and a large atmospheric mixing angle is single right-handed neutrino dominance [4]. See also [5, 6]. It is also possible to account for a large solar neutrino angle in this framework [7]. For example a large solar angle may result from sequential right-handed neutrino dominance due to the leading sub-dominance of a second right-handed neutrino [7], leading to a full neutrino mass hierarchy  $m_1 \ll m_2 \ll m_3$ .

In charged lepton interactions of the Standard Model the lepton flavour violation (LFV) is suppressed by the heavy see-saw mass scale, or equivalently the small left-handed Majorana masses, and is practically unobservable. However in low energy supersymmetric (SUSY) theories the situation dramatically changes for the better. In SUSY the LFV is imprinted on the slepton mass matrices, resulting in slepton masses which are off-diagonal in flavour space. The off-diagonal slepton masses can

then induce LFV in loops suppressed only by the SUSY breaking scale, multiplied by ratios of the off-diagonal slepton mass to the diagonal slepton mass [9, 10, 11, 12].

The experimental prospects for improving the limits or actually measuring LFV processes are very promising. The 90% C.L. limits of  $\text{BR}(\tau \rightarrow \mu\gamma) < 1.1 \times 10^{-6}$  [13] and  $\text{BR}(\mu \rightarrow e\gamma) < 1.2 \times 10^{-11}$  [14] are particularly stringent in constraining SUSY models. In fact, these limits will be lowered in the next 2-3 years as the present B factories, inevitably producing tau leptons along with the b quarks, will collect 15-20 times more data and as the new  $\mu \rightarrow e\gamma$  experiment at PSI probes the branching ratio down to  $10^{-14}$  [15, 16]. The forthcoming experimental results are clearly a powerful incentive for theoretical studies of  $\tau \rightarrow \mu\gamma$  and  $\mu \rightarrow e\gamma$ , and this provides an important underlying motivation for the present paper. It should be noted however that LFV violation can originate from other effects unrelated to the see-saw mechanism, for example colour triplet scalars in GUT models, or off-diagonal slepton masses generated from flavour violating effects in the SUSY breaking sector. In any observation of LFV, such effects would need to be disentangled from the effects due to the see-saw mechanism in the CMSSM considered here.

There is a huge literature on LFV in the framework of the CMSSM, where the constraint of universal scalar mass  $m_0$  and trilinear mass  $A_0$  implies that the slepton mass non-universality originates entirely from RG effects due to right-handed neutrinos between the GUT scale and the lightest right-handed neutrino mass scale [17]. There is a much smaller literature concerned with LFV in models based on single right-handed neutrino dominance [18, 19]. In our previous paper [18] we made the important observation that a large  $\tau \rightarrow \mu\gamma$  rate results from models in which the dominant right-handed neutrino is the heaviest one, and the neutrino Yukawa matrix has a lop-sided form with an order unity Yukawa coupling in the 23 position of the

matrix

$$Y^\nu \approx \begin{pmatrix} 0 & 0 & 0 \\ 0 & 0 & 1 \\ 0 & 0 & 1 \end{pmatrix}.$$

In subsequent papers [19] a bottom-up analysis of various types of right-handed neutrino dominance was discussed and  $\tau \rightarrow \mu\gamma$  and  $\mu \rightarrow e\gamma$  were both considered in terms of coefficients  $C_{ij}$  which parametrise the off-diagonal slepton masses to leading log approximation in the mass insertion approach to LFV. Bounds on the coefficients  $C_{ij}$  were presented as a function of the sneutrino and second gaugino masses  $m_{\tilde{\nu}}$  and  $M_2$ , and  $C_{ij}$  were related to Yukawa couplings and right-handed neutrino masses for each of the different types of right-handed neutrino dominance [19].

In the present paper we provide a dedicated analysis of a particular class of right-handed neutrino dominance models, namely sequential dominance (SD). The reason why we choose to focus on SD is that it provides a particularly elegant application of the see-saw mechanism to the LMA MSW solution, and these are the only models where a full neutrino mass hierarchy  $m_1 \ll m_2 \ll m_3$  arises naturally. Another attractive feature of SD models is that it may become possible to relate the rate for  $\mu \rightarrow e\gamma$  directly to the sub-leading Yukawa couplings. We shall discuss the conditions under which this may be possible later. There are several examples of models in the literature which rely on SD [20, 5, 21, 22]. In the realistic models the dominant right-handed neutrino is either the heaviest or the lightest. We refer these cases as heavy sequential dominance (HSD) or light sequential dominance (LSD), respectively, and discuss these cases separately.

In this paper, then, we perform a global analysis of HSD and LSD models in the framework of the CMSSM, presenting our predictions in the  $(m_0, M_{1/2})$  plane, assuming radiative electroweak symmetry breaking, and including all observed laboratory data. We give predictions for branching fractions for  $\tau \rightarrow \mu\gamma$  and  $\mu \rightarrow e\gamma$  in terms of a convenient parametrisation which we introduce for the neutrino Yukawa couplings.

Our results confirm that the  $\tau \rightarrow \mu\gamma$  rate distinguishes HSD from LSD. We further show that the  $\mu \rightarrow e\gamma$  rate may allow a determination of the sub-dominant neutrino Yukawa couplings in the flavour basis, in terms of an expansion parameter  $\lambda$ . We show that measurement of  $\theta_{13}$  may determine a ratio of sub-dominant Yukawa couplings. We discuss quantitative effects which were not present in the leading log and leading mass insertion approximations of [19], for example cases where  $\mu \rightarrow e\gamma$  is controlled by the 13 slepton mass.

The remainder of the paper is set out as follows. In section 2 we discuss sequential dominance and introduce our parametrisation. We also make some leading log analytic estimates of off-diagonal slepton masses in terms of this parametrisation, and discuss the implications for LFV processes. In section 3 we give our full numerical results.

## 2 Sequential Dominance

### 2.1 Brief Review

In this subsection we give a brief review of SD, including the analytic estimates of neutrino masses and mixing angles in terms of Yukawa couplings and right-handed neutrino masses, which we assume here to be real. More details can be found in [8]. Note that all the results in this subsection are independent of the mass ordering of right-handed neutrino masses, and so apply to both HSD and LSD.

In the flavour basis where the charged lepton mass matrix is diagonal, the diagonal right-handed neutrino mass matrix is written as

$$M_{RR} = \begin{pmatrix} X' & 0 & 0 \\ 0 & X & 0 \\ 0 & 0 & Y \end{pmatrix} \quad (3)$$

and the neutrino Yukawa matrix without loss of generality as

$$Y_{LR}^\nu = \begin{pmatrix} a' & a & d \\ b' & b & e \\ c' & c & f \end{pmatrix}. \quad (4)$$

In order to account for a neutrino mass hierarchy and large neutrino mixing angles in a natural way (without fine-tuning) the following SD condition was proposed [7],

$$\frac{|e^2|, |f^2|, |ef|}{Y} \gg \frac{|xy|}{X} \gg \frac{|x'y'|}{X'} \quad (5)$$

where  $x, y \in \{a, b, c\}$  and  $x', y' \in \{a', b', c'\}$ . It is further assumed [4] that

$$d \ll e \approx f. \quad (6)$$

Then it was shown that the neutrino masses are given to leading order in  $m_2/m_3$  by [8],

$$\begin{aligned} m_1 &\sim O\left(\frac{x'y'}{X'} v_2^2\right) \\ m_2 &\approx \frac{a^2 + (c_{23}b - s_{23}c)^2}{X} v_2^2 \\ m_3 &\approx \frac{e^2 + f^2}{Y} v_2^2 \end{aligned} \quad (7)$$

where  $v_2$  is a Higgs vacuum expectation value (vev) associated with the (second) Higgs doublet that couples to the neutrinos. Note that with SD each neutrino mass is generated by a separate right-handed neutrino, and the origin of the neutrino mass hierarchy is thus linked to the sequential condition in Eq.5. The neutrino mixing angles are given to leading order in  $m_2/m_3$  by [8],

$$\begin{aligned} \tan \theta_{23} &\approx \frac{e}{f} \\ \tan \theta_{12} &\approx \frac{a}{(c_{23}b - s_{23}c)} \\ \theta_{13} &\approx \frac{a(s_{23}b + c_{23}c)}{(e^2 + f^2)} \frac{Y}{X} \end{aligned} \quad (8)$$

Thus, assuming SD, the atmospheric angle is given by a ratio of dominant right-handed neutrino couplings associated with  $Y$ , the solar angle is given by a ratio of

sub-dominant right-handed neutrino couplings associated with  $X$ , and  $\theta_{13}$  is of order  $m_2/m_3$ . The sub-sub-dominant right-handed neutrino  $X'$  with couplings  $a', b', c'$  is completely irrelevant for neutrino physics unless  $m_1$  can be measured. In writing the equation for  $\theta_{13}$  we have assumed for simplicity that

$$d \ll a(s_{23}b + c_{23}c)Y/(\sqrt{e^2 + f^2}X). \quad (9)$$

At leading order in a mass insertion approximation [9, 11] the branching fractions of LFV processes are given by

$$\text{BR}(l_i \rightarrow l_j \gamma) \approx \frac{\alpha^3}{G_F^2} f(M_2, \mu, m_{\tilde{\nu}}) |m_{\tilde{L}_{ij}}^2|^2 \xi_{ij} \tan^2 \beta \quad (10)$$

where  $l_1 = e, l_2 = \mu, l_3 = \tau$ , and where the off-diagonal slepton doublet mass squared is given in the leading log approximation (LLA) by

$$m_{\tilde{L}_{ij}}^{2(LLA)} \approx -\frac{(3m_0^2 + A_0^2)}{8\pi^2} C_{ij} \quad (11)$$

where the leading log coefficients are given by

$$\begin{aligned} C_{21} &= a'b' \ln \frac{M_U}{X'} + ab \ln \frac{M_U}{X} + de \ln \frac{M_U}{Y} \\ C_{32} &= b'c' \ln \frac{M_U}{X'} + bc \ln \frac{M_U}{X} + ef \ln \frac{M_U}{Y} \\ C_{31} &= a'c' \ln \frac{M_U}{X'} + ac \ln \frac{M_U}{X} + df \ln \frac{M_U}{Y} \end{aligned} \quad (12)$$

The factors  $\xi_{ij}$  in Eq.10 represent the ratio of the leptonic partial width to the total width,

$$\xi_{ij} = \frac{\Gamma(l_i \rightarrow l_j \nu_i \bar{\nu}_j)}{\Gamma(l_i \rightarrow \text{all})} \quad (13)$$

Clearly  $\xi_{21} = 1$  but  $\xi_{32}$  is non-zero and must be included for correct comparison with the experimental limit on the branching ratio for  $\tau \rightarrow \mu\gamma$ . This factor is frequently forgotten in the theoretical literature.

We shall focus on  $C_{21}$  and  $C_{32}$  which correspond to  $\mu \rightarrow e\gamma$  and  $\tau \rightarrow \mu\gamma$ . For HSD the couplings  $a', b', c'$  are expected to be smaller than the couplings  $a, b, c$ , and we will

therefore drop them in both our analytic and numerical analysis. For LSD the primed terms are also not relevant for LFV since as discussed later we will set  $X' = M_U$  which means that this right-handed neutrino is immediately decoupled at the GUT scale, and so  $\ln \frac{M_U}{X'} = 0$ . In the case of LSD this is rather a strong assumption and if  $X' < M_U$  these Yukawa couplings will again become relevant. Dropping the primed contributions for both HSD and LSD the relevant coefficients are then given by

$$\begin{aligned} C_{21} &= ab \ln \frac{M_U}{X} + de \ln \frac{M_U}{Y} \\ C_{32} &= bc \ln \frac{M_U}{X} + ef \ln \frac{M_U}{Y} \end{aligned} \quad (14)$$

Note that the primed couplings are irrelevant to either the neutrino masses and mixing angles or the LFV processes. This applies to both the HSD and the LSD cases.

## 2.2 A convenient parametrisation

The above analytic results for the neutrino masses and mixing angles suggest the following parametrisation of the Yukawa couplings and right-handed neutrino masses in terms of order unity coefficients  $a_{ij}$  and  $A$ , together with an expansion parameter  $\lambda$  raised to integer powers,

$$\begin{aligned} a &\equiv a_{12}\lambda^n f \\ b &\equiv a_{22}\lambda^n f \\ c &\equiv a_{32}\lambda^n f \\ d &\equiv a_{13}\lambda^m f \\ e &\equiv a_{23}f \\ X &\equiv A\lambda^{2n-1}Y \end{aligned} \quad (15)$$

where

$$\lambda \equiv \sqrt{\frac{|\Delta m_{21}^2|}{|\Delta m_{32}^2|}} \approx 0.15. \quad (16)$$

Currently the data prefers  $\lambda \approx 0.15$ , with large uncertainty. It is the smallness of this value that is the motivation for sequential dominance.

In terms of the parametrisation in Eq.15, the neutrino mixing angles in Eq.8 become,

$$\begin{aligned} \tan \theta_{23} &\approx a_{23} \\ \tan \theta_{12} &\approx \frac{a_{12}}{a_{22}(c_{23} - s_{23}r)} \\ \theta_{13} &\approx \frac{\lambda a_{12}a_{22}(s_{23} + c_{23}r)}{A(1 + a_{23}^2)} \end{aligned} \quad (17)$$

where for convenience we have also defined the following ratio of sub-dominant Yukawa couplings which clearly plays a crucial role in determining  $\theta_{13}$ ,

$$r = \frac{c}{b} = \frac{a_{32}}{a_{22}}. \quad (18)$$

The motivation for the above parametrisation is that it reproduces the large atmospheric and solar mixing angles  $\tan \theta_{23} \sim 1$ ,  $\tan \theta_{12} \sim 1$ , with the dimensionless parameters  $a_{ij}$  being of order unity.<sup>1</sup>

Similarly the neutrino masses in Eq.7 become, in terms of the parametrisation in Eq.15,

$$\begin{aligned} m_1 &\approx 0 \\ m_2 &\approx (a_{12}^2 + a_{22}^2(c_{23} - s_{23}r)^2) \frac{\lambda f^2}{AY} \\ m_3 &\approx (1 + a_{23}^2) \frac{f^2}{Y} \end{aligned} \quad (19)$$

The ratio of second and third neutrino masses is then  $m_2/m_3 \sim \lambda$  which motivates the definition of the expansion parameter in Eq.16. A further motivation for this

---

<sup>1</sup>Note that with all  $a_{ij}$  and  $A$  of order unity this is not the most general parametrisation that satisfies the conditions in Eqs.5,6 that define this class of models. Also note that as before we have assumed for simplicity that  $d$  is small in the equation for  $\theta_{13}$ , and the condition for this is now  $m \geq 2$ .

parametrisation is that it clearly shows that the neutrino masses and mixing angles in Eq.19, 17 are completely independent of  $n$ . Although the neutrino masses and mixings cannot determine the choice of integer  $n$ , which controls the magnitude of the Yukawa couplings, the LFV processes are able to do so as we now discuss.

Using our parametrisations in Eq.15 the coefficients relevant for  $\mu \rightarrow e\gamma$  and  $\tau \rightarrow \mu\gamma$  from Eq.14 are then determined by the products of Yukawa couplings

$$\begin{aligned} ab &= a_{12}a_{22}\lambda^{2n}f^2 \\ de &= a_{13}a_{23}\lambda^m f^2 \\ bc &= a_{22}^2 r \lambda^{2n} f^2 \\ ef &= a_{23}f^2 \end{aligned} \tag{20}$$

Then from Eqs.14, 20 we have

$$\begin{aligned} C_{21} &= a_{12}a_{22}\lambda^{2n}f^2 \ln \frac{M_U}{X} + a_{13}a_{23}\lambda^m f^2 \ln \frac{M_U}{Y} \\ C_{32} &= a_{22}^2 r \lambda^{2n} f^2 \ln \frac{M_U}{X} + a_{23}f^2 \ln \frac{M_U}{Y} \end{aligned} \tag{21}$$

The coefficients  $C_{ij}$  which determine the strength of LFV processes are clearly governed by the value of the Yukawa coupling  $f$  together with the integers  $n, m$  which control the magnitudes of the Yukawa couplings. The values of the right-handed neutrino masses does not directly influence the coefficients  $C_{ij}$  very much, with only a mild logarithmic dependence. However the values of the right-handed neutrino masses will have an important indirect effect on LFV processes via the values of the Yukawa couplings. For example for a fixed  $m_3$ ,  $C_{32} \propto f^2 \propto Y$ , so the  $\tau \rightarrow \mu\gamma$  rate increases as the dominant right-handed neutrino mass  $Y$  becomes heavier [18]. We shall now discuss the two cases HSD and LSD separately, corresponding to the dominant right-handed neutrino of mass  $Y$  being the heaviest or the lightest, respectively.

## 2.3 Heavy Sequential Dominance (HSD)

HSD is defined by the condition that the dominant right-handed neutrino of mass  $Y$  is the heaviest, with

$$Y \gg X \gg X' \quad (22)$$

Typically in unified models the heaviest right-handed neutrino is in the 33 position and the 33 element of the neutrino Yukawa matrix is equal to the top quark Yukawa coupling  $f = h_t$  (at the high energy scale). The HSD case then leads to the “lopsided” form of neutrino Yukawa matrix with an order unity Yukawa coupling in the 23 position, and subsequently a large expected rate for  $\tau \rightarrow \mu\gamma$  [18]. For HSD with  $f = h_t$ , the atmospheric neutrino mass  $m_3 \approx \sqrt{|\Delta m_{32}^2|}$  then implies that the heaviest (dominant) right-handed neutrino has mass

$$Y \approx 2m_t^2/m_3 \approx 3 \times 10^{14} \text{GeV.} \quad (23)$$

where we have used the GUT scale value of the top quark mass  $m_t$  which for large  $\tan\beta$  is about 0.7 times its low energy value. For HSD the condition that  $X \ll Y$  implies, from Eq.15, that

$$n \geq 1 \quad (24)$$

Recall that we also assumed  $m \geq 2$ . The neutrino matrices in Eqs.3,4, in terms of the parametrisation in Eq.15, are summarised below for the case of HSD,

$$M_{RR}^{HSD} = \begin{pmatrix} - & 0 & 0 \\ 0 & A\lambda^{2n-1} & 0 \\ 0 & 0 & 1 \end{pmatrix} Y \quad (25)$$

$$Y_{LR}^{\nu HSD} = \begin{pmatrix} - & a_{12}\lambda^n & a_{13}\lambda^m \\ - & a_{22}\lambda^n & a_{23} \\ - & ra_{22}\lambda^n & 1 \end{pmatrix} h_t \quad (26)$$

where the blanks indicate entries which are irrelevant for both neutrino masses and mixing angles and LFV. The neutrino masses and mixing angles are given by Eqs.17,19, independently of  $n$ .

In this case it is clear from Eq.21 that  $\tau \rightarrow \mu\gamma$ , which corresponds to  $C_{32}$ , is large and independent of  $n$ , being given approximately by

$$C_{32} = a_{22}h_t^2 \ln \frac{M_U}{Y} \quad (27)$$

On the other hand  $\mu \rightarrow e\gamma$ , which corresponds to  $C_{21}$ , is smaller and more model dependent since it depends on the integers  $n, m$ ,

$$C_{21} = a_{12}a_{22}\lambda^{2n}h_t^2 \ln \frac{M_U}{X} + a_{13}a_{23}\lambda^m h_t^2 \ln \frac{M_U}{Y} \quad (28)$$

From our numerical results we shall find that the experimental limit on  $\mu \rightarrow e\gamma$  will require  $n \geq 2$ . Since  $ab \sim \lambda^{2n}$  while  $de \sim \lambda^m$ , if  $2n < m$  then  $ab$  will dominate over  $de$ , while if  $2n > m$  then  $de$  will dominate over  $ab$ . In the second case  $\mu \rightarrow e\gamma$  is controlled by the 13 neutrino Yukawa coupling  $d$ . We emphasise the fact that although  $\mu \rightarrow e\gamma$  is model dependent in this framework we understand precisely its origin.

## 2.4 Light Sequential Dominance (LSD)

LSD is defined by the condition that the dominant right-handed neutrino of mass  $Y$  is the lightest, with

$$X' \gg X \gg Y \quad (29)$$

The LSD case then leads a more “symmetrical” form of neutrino Yukawa matrix with no large off-diagonal Yukawa couplings, and hence a small expected rate for  $\tau \rightarrow \mu\gamma$ . Such a form of neutrino Yukawa matrix is consistent with an exactly symmetrical or anti-symmetrical or mixed symmetry form, or some more general matrix with small off-diagonal couplings. LSD is more complicated to discuss since we need to re-order the matrices in Eqs.3,4, to put the heaviest right-handed neutrino of mass  $X'$  in the third column. Then we shall make a similar assumption for LSD that the 33 element of the neutrino mass matrix to be equal to the top quark Yukawa coupling  $c' = h_t$ .

For LSD to set the scale of the right-handed neutrino masses, we need to relate the dominant right-handed neutrino Yukawa coupling  $f$  to  $c' = h_t$ . In particular, we extend our parametrisation to include

$$f = a_{31} \lambda^p c' \quad (30)$$

where  $p > 0$ , and  $a_{31}$  is an order unity coefficient. For LSD with  $c' = h_t$ , the atmospheric neutrino mass  $m_3 \approx \sqrt{|\Delta m_{32}^2|}$  then implies that the lightest (dominant) right-handed neutrino has mass

$$Y \approx a_{31}^2 \lambda^{2p} 3 \times 10^{14} \text{GeV}. \quad (31)$$

with  $p > 0$ . The sub-dominant right-handed neutrino mass is heavier than  $Y$  and its mass is parametrised by

$$X = A \lambda^{2n-1} Y \approx A a_{31}^2 \lambda^{2p+2n-1} 3 \times 10^{14} \text{GeV} \quad (32)$$

with,

$$n \leq 0 < p. \quad (33)$$

In LSD the heaviest right-handed neutrino mass is  $X'$  which must be heavy enough to satisfy the sequential condition, corresponding to the second inequality in Eq.5,

$$\frac{|xy|}{X} \gg \frac{c'^2}{X'} \quad (34)$$

From Eqs.15,32,34 we find

$$X' \gg \lambda^{-1} 3 \times 10^{14} \text{GeV} \quad (35)$$

independently of  $p, n$ . Eq.35 implies that  $X'$  cannot be (much) below the GUT scale  $M_U$ . As indicated earlier we shall assume  $X' = M_U$  which implies that there can be no LFV effects arising from this right-handed neutrino. In order to ensure that  $X \ll X'$  by comparing Eqs.32 and 35 we also have the condition

$$p + n > 0 \quad (36)$$

The neutrino matrices in Eqs.3,4, in terms of the parametrisation in Eqs.15,30 are summarised below for the case of LSD, after re-ordering them to put the heaviest right-handed neutrino in the third column, and the lightest (dominant) right-handed neutrino in the first column,

$$M_{RR}^{LSD} = \begin{pmatrix} a_{31}^2 \lambda^{2p} & 0 & 0 \\ 0 & Aa_{31}^2 \lambda^{2p+2n-1} & 0 \\ 0 & 0 & - \end{pmatrix} 3 \times 10^{14} GeV \quad (37)$$

$$Y_{LR}^{\nu LSD} = \begin{pmatrix} a_{13}a_{31}\lambda^{p+m} & a_{12}a_{31}\lambda^{p+n} & - \\ a_{23}a_{31}\lambda^p & a_{22}a_{31}\lambda^{p+n} & - \\ a_{31}\lambda^p & ra_{22}a_{31}\lambda^{p+n} & 1 \end{pmatrix} h_t \quad (38)$$

where the blanks indicate entries which are irrelevant if  $X' = M_U$ . However, as we mentioned previously, if  $X' < M_U$  such Yukawa couplings will again become important. Note that  $n$  is a non-positive integer, and in realistic models it is nearly always negative so that the Yukawa couplings in the first column are smaller than the Yukawas in the second column. The advantage of this parametrisation is that it provides a unified parametrisation of HSD and LSD, with  $n$  being positive for HSD, and negative or zero for LSD. In this unified parametrisation the neutrino masses and mixing angles are still given by the same formulas as in Eqs.17,19, independently of  $n, p, a_{31}$ .

In this case it is clear from Eq.21 that  $\tau \rightarrow \mu\gamma$ , which corresponds to  $C_{32}$ , is now much smaller and model dependent since it depends on the integers  $p, n$ ,

$$C_{32} = ra_{22}^2 a_{31}^2 \lambda^{2p+2n} h_t^2 \ln \frac{M_U}{X} + a_{22} a_{31}^2 \lambda^{2p} h_t^2 \ln \frac{M_U}{Y} \quad (39)$$

If  $n < 0$  then, in the notation of Eq.20,  $bc$  dominates over  $ef$ . Turning to  $\mu \rightarrow e\gamma$ , which corresponds to  $C_{21}$ , since  $n \leq 0$  while  $m \geq 2$  we have approximately,

$$C_{21} = a_{12} a_{22} a_{31}^2 \lambda^{2p+2n} h_t^2 \ln \frac{M_U}{X} \quad (40)$$

so that, in the notation of Eq.20,  $ab$  always dominates over  $de$ . By comparing Eqs.39 to 40, we see that in all cases

$$C_{32} \sim C_{21} \sim \lambda^{2p+2n} h_t^2 \ln \frac{M_U}{X} \quad (41)$$

which leads to the LSD prediction that the branching fractions for  $\tau \rightarrow \mu\gamma$  and  $\mu \rightarrow e\gamma$  should be comparable, and are controlled by the value of  $p + n$ . We already saw in Eq.36 that  $X \ll X'$  requires  $p + n > 0$ . We shall see in the next section that the experimental limit on  $\mu \rightarrow e\gamma$  will require  $p + n \geq 2$ . This implies that the  $\tau \rightarrow \mu\gamma$  rate for LSD is suppressed relative to that for HSD by of order  $\lambda^8$  or more, which effectively makes  $\tau \rightarrow \mu\gamma$  unobservable in this case. In the case that  $X' < M_U$  and the 23 Yukawa coupling were set equal to the 32 Yukawa coupling we would find

$$C_{32} \sim \lambda^{p+n} h_t^2 \ln \frac{M_U}{X'} \quad (42)$$

which would imply that the  $\tau \rightarrow \mu\gamma$  rate for LSD is suppressed relative to that for HSD by of order  $\lambda^4$  or more, which is still at least three orders of magnitude below current limits.

### 3 Numerical Results

Our numerical results are based on the top-down global analysis of the CMSSM with universal soft scalar mass  $m_0$ , soft gaugino mass  $M_{1/2}$ , soft trilinear mass  $A_0$  and the sign of the Higgs superpotential mass parameter  $\mu$  which we take to be positive as implied by the recent muon anomalous magnetic moment measurement. In a standard notation [23] the complete list of the input parameters varied at the unification scale  $M_U \approx 2 \times 10^{16}$  GeV (which itself is allowed to vary) contains the soft masses  $m_0$ ,  $M_{1/2}$ ,  $A_0$ , the unified gauge coupling  $\alpha_U$ , the deviation of the QCD gauge coupling  $\alpha_3$  from  $\alpha_U$ ,  $\epsilon_3 \equiv (\alpha_3 - \alpha_U)/\alpha_U$ , the deviation of the  $b, \tau$  Yukawa couplings  $h_{b,\tau}$  from the (varying) top Yukawa coupling  $h_t$ ,  $\epsilon_{b,\tau} = (h_{b,\tau} - h_t)/h_t$ , and the five parameters of the neutrino sector  $Y$ ,  $a_{12}$ ,  $a_{22}$ ,  $a_{23}$  and  $A$  defined earlier. The five neutrino parameters are only allowed to vary within 20 – 30% (see Eq.15) but typically good fits are obtained for values in the smaller range  $\sim 10\%$  which means that  $Y$  and the  $a$ 's stay

close to  $3 \times 10^{14}$ GeV and 1, respectively.  $r = a_{32}/a_{22}$  is held fixed in the analysis.<sup>2</sup>  $\mu$  is an input parameter at the low scale which we take as the  $M_Z$  scale. The function  $\chi^2 = \sum(x_i^{CMSSM} - x_i^{exp})^2/\sigma_i^2$  is evaluated based on the following observables  $x_i$ :  $\alpha$ ,  $G_\mu$ ,  $\alpha_3(M_Z)$ ,  $M_t$ ,  $m_b(m_b)$ ,  $M_\tau$ ,  $M_Z$ ,  $M_W$ ,  $\Delta\rho$ ,  $BR(b \rightarrow s\gamma)$ ,  $a_\mu^{\text{NEW}}$  and the neutrino mass differences and mixing angles of Eqs.(1) and (2). The low-scale value of the bilinear parameter  $B\mu$  is directly related to ratio of Higgs vacuum expectation values  $\tan\beta$  and the latter is kept fixed in the analysis. Each computed charged fermion mass includes the complete 1-loop SUSY threshold correction and correct radiative electroweak symmetry breaking at one loop is required at all points by adopting tight  $\sigma_{M_Z}$  and  $\sigma_{M_W}$ . A direct search limit is applied to the mass of each unobserved particle including  $m_{h^0} > 114$ GeV. We shall present our results as contours in the  $(m_0, M_{1/2})$  plane, for fixed  $\tan\beta$ , with  $A_0$  and  $|\mu|$  varying over the plane. More details of the global analysis can be found in [23] and [24].<sup>3</sup>

The main constraint of the present study comes from the muon  $g - 2$ . Based on [25, 26] we require the contribution from new physics to fit

$$a_\mu^{\text{NEW}} = a_\mu^{(\text{exp})} - a_\mu^{\text{SM}} = (34 \pm 11) \times 10^{-10}. \quad (43)$$

The main focus of the analysis is neutrino masses and mixing angles which we fit to the central atmospheric and LMA MSW values.  $\theta_{13}$  is predicted in terms of a ratio of Yukawa couplings as discussed above and computed from the exact form of the MNS matrix obtained at low energy. We emphasise that the neutrino parameter fit is within the framework of SD, and in this framework it becomes possible to make direct connections between LFV processes and specific Yukawa couplings, subject to the conditions discussed in sections 2.3 and 2.4. This would not be possible for

---

<sup>2</sup>We study cases with  $r$  taking on different values as explained below.

<sup>3</sup>We note that in the presented top-down analysis the first and second generation quark and charged lepton masses and CKM elements are always fit very well in a separate minimisation with small first and second generation yukawa couplings as input at  $M_U$ . The presence of the  $3 \times 3$  yukawa matrices  $Y^u$ ,  $Y^d$  and diagonal  $Y^e$  renders the whole analysis more complete and consistent while, at the same time, the additional flavour structure of  $Y^u$  and  $Y^d$  has no effect on the rest of the analysis.

example if the hierarchy resulted from the tuning of parameters. It is also worth noting that we perform a careful RG analysis, adjusting the RG evolution below each right-handed neutrino mass threshold, and also perform an exact one-loop calculation of lepton flavour violating processes. Thus we have very accurate predictions for the  $\tau \rightarrow \mu\gamma$  and  $\mu \rightarrow e\gamma$  experiments which is increasingly important due to the experimental progress. We shall compare our results to the leading log and mass insertion approximations described in the previous sections, and in some cases find large discrepancies.

In Figure 1 we show the results of a global analysis of the HSD model for  $\tan \beta = 50$ ,  $n = 2$ ,  $r = -1$ ,  $a_{13} = 0$ , and the parameters refer to the matrices in Eq.25,26. This choice of parameters we call the “baseline” parameter set. Figure 1(a) shows the global  $\chi^2$  fit across the  $(m_0, M_{1/2})$  plane, with the best fit in the region  $m_0 \sim M_{1/2} \sim 500$  GeV. The fit deteriorates for large  $M_{1/2}$  and  $m_0$  because of the muon anomalous magnetic moment which is shown in the panel (b) and for small  $M_{1/2}$  and small  $m_0$  because of  $b \rightarrow s\gamma$ . In the first case the sparticles are too heavy to generate the observed discrepancy (43) while in the latter case they are too light making the chargino contribution to the  $b \rightarrow s\gamma$  effective amplitude too large.

In Figure 2 we show the predictions of the HSD model with the baseline parameters for the branching ratios of  $\tau \rightarrow \mu\gamma$  and  $\mu \rightarrow e\gamma$ . As expected from Eqs.27 and 28 the upper panels show a large rate for (a)  $\tau \rightarrow \mu\gamma$  and (b)  $\mu \rightarrow e\gamma$  close to the current limits. The prediction for the large  $\tau \rightarrow \mu\gamma$  rate in panel (a) is quite a robust prediction of HSD [18]. As discussed later the predictions are expected to scale as  $\tan^2 \beta$ . The  $\mu \rightarrow e\gamma$  rate in panel (b) is sensitive to the choice of  $n$ , which we have taken to be  $n = 2$ . This rate can easily be enhanced by taking smaller  $n$  or suppressed by taking larger  $n$ , as is clear from Eq.28. In the lower panels of Figure 2 we investigate the accuracy of the leading log approximation (LLA) used to calculate the off-diagonal slepton masses in Eq.11, with the HSD coefficients in Eqs.27,28, as

compared to the exact numerical calculation used to generate our numerical results. We define the fractional error as follows:

$$\Delta_{ij} \equiv \frac{m_{\tilde{L}_{ij}}^{2(LLA)} - m_{\tilde{L}_{ij}}^2}{m_{\tilde{L}_{ij}}^2} \quad (44)$$

Figure 2(c) shows contours of  $\Delta_{32}$  while panel (d) shows  $\Delta_{21}$ , in each case giving a measure of the error that would have been incurred had the LLA been used in calculating the rates for  $\tau \rightarrow \mu\gamma$  and  $\mu \rightarrow e\gamma$ . The rates shown in the upper panels were, of course, calculated exactly without using the LLA approximation. The LLA can induce errors of up to 50% for the lighter SUSY masses. Note that the errors double for the branching ratio.

The parameter dependence of  $\text{BR}(\mu \rightarrow e\gamma)$  in the HSD model is examined in Figure 3, where in each case we allow one or two parameters to change from the baseline parameter set used in Figures 1 and 2, in order to illustrate a particular effect. In Figure 3(a), we suppress the subdominant Yukawa couplings by taking  $n = 4$ , leaving all the other baseline parameters unchanged. As expected from Eq.28, this has the effect of suppressing  $\text{BR}(\mu \rightarrow e\gamma)$  by a relative factor of  $\lambda^8 \approx 2.5 \times 10^{-7}$  compared to the previous result, which approximately corresponds to what is observed by comparing Figure 3(a) to Figure 2(b). This result demonstrates how sensitive  $\text{BR}(\mu \rightarrow e\gamma)$  is to the values of the subdominant Yukawa couplings of order  $\lambda^n$ , with the prospect that a measurement of this rate is equivalent to a measurement of these Yukawa couplings parametrised by  $n$ . This is an exciting prospect offered by the SD class of models, however this result is subject to the discussion below Eq.28, which we shall return after the following paragraph.

We now discuss the numerical importance of effects beyond the leading mass insertion approximation. In Figure 3(b) we set  $a_{22} = 0$  with the other parameters as in the baseline set, in particular  $a_{13} = 0$ . Having  $a_{22} = a_{13} = 0$  should completely kill  $\mu \rightarrow e\gamma$  according to Eq.28, however clearly it does not, since the rate in Figure 3(b)

is in fact larger than the rate in Figure 3(a) by three orders of magnitude! Clearly the mass insertion approximation, on which our analytic expectations of the previous section, and all the results in [19] for example, are based, is no longer reliable in the limit of  $a_{22} = a_{13} = 0$ . We note that having  $a_{22} = a_{13} = 0$  is completely reasonable from the SD point of view of neutrino masses and mixing angles, and would correspond to some specific type of texture of the “Fritzsch” type [27] for example. Although in this case  $C_{21} = 0$ , the values of  $C_{32}$  and  $C_{31}$  are non-zero, leading to off-diagonal 32 and 31 slepton masses, where according to Eq.12 the 31 slepton mass must be arising from the  $ac$  product of Yukawa couplings which would be suppressed by increasing  $n$ . A 21 flavour violation may be generated by a double mass insertion involving both 32 and 31, and this results in the observed rate for  $\mu \rightarrow e\gamma$  in panel (b) of Figure 3, although we calculate the rate exactly without relying on any mass insertion methods at all as in [12, 18], for example. We call this the 13 slepton effect.

We now consider the effects of the 13 Yukawa coupling which contribute to  $\text{BR}(\mu \rightarrow e\gamma)$  according to the second term of Eq.28. Such effects are illustrated in Figure 3(c) where we keep  $n = 4$  as in panel (a), but now take  $a_{13}$  to be of order one, with the 13 Yukawa coupling controlled by the value of  $m$ , which we take to be  $m = 3$ . Switching on the 13 Yukawa coupling in Figure 3(c) results in a dramatic increase in  $\text{BR}(\mu \rightarrow e\gamma)$  compared to Figure 3(a). We call this the 13 Yukawa effect.

Figure 3(d) shows  $\text{BR}(\mu \rightarrow e\gamma)$  in the HSD model where  $\tan\beta = 10$  and the remaining parameters take the baseline values. Comparing to the baseline contours in Figure 1(b), it is clear that the contours do not simply scale as  $\tan^2\beta$ . The reason is that  $|\mu|$  is fixed by electroweak symmetry breaking, and also depends on  $\tan\beta$ , and this leads to the difference in the two sets of contours. If  $|\mu|$  were held fixed then we would find the expected  $\tan^2\beta$  scaling of the rates. The figures illustrate the importance of the implicit  $|\mu|$  dependence for differing values of  $\tan\beta$ , and warn against naively assuming a  $\tan^2\beta$  scaling of the results in the  $(m_0, M_{1/2})$  plane.

In Figure 4 we show the prediction of  $\sin^2 2\theta_{13}$  as a function of the ratio of sub-dominant Yukawa couplings  $r = a_{32}/a_{22}$  for the HSD class of models, taking all the other parameters equal to their baseline values, in particular  $a_{13} = 0$ . The qualitative variation of this angle with  $r$  follows from Eq.17 which shows that although the natural value of the angle  $\theta_{13}$  is set by the parameter  $\lambda$ , as  $r \rightarrow -1$ ,  $\theta_{13} \rightarrow 0$ , while maintaining  $\tan \theta_{12} \sim 1$ . Numerically we perform a global fit for three specific values of  $r$  and for each value we find a band of values of  $\sin^2 2\theta_{13}$  corresponding to the variation in the values of the order one coefficients. For  $r = -1$  the value of  $\sin^2 2\theta_{13}$  is not exactly equal to zero, due to subleading effects beyond the level of approximation of Eq.17, but it does get very small. In general it is fair to say that over most of the range of  $r$  the value of  $\sin^2 2\theta_{13}$  is below the current CHOOZ limit of about 0.14 but for  $r > 0$  it should be within the combined ICARUS and OPERA expected 2009 limit of 0.03. However it is clear that for  $r < 0$  a measurement of  $\sin^2 2\theta_{13}$  would only be possible at JHF or a Neutrino Factory. Note that Figure 4 assumes  $a_{13} = 0$ , and the result is more complicated if this is not the case. We emphasise that for  $a_{13} = 0$  the rate for  $\mu \rightarrow e\gamma$  is generally independent of the prediction for  $\theta_{13}$ , which is clear analytically by comparing Eq.17 to Eq.28. The point is simply that  $C_{21}$  is independent of  $a_{32}$  and hence  $r$ . <sup>4</sup> We emphasise that  $\theta_{13}$  can be rather large while  $\mu \rightarrow e\gamma$  can be arbitrarily suppressed simply by increasing the value of  $n$ .

In Figure 5 we show predictions of the LSD model for the branching ratios of  $\tau \rightarrow \mu\gamma$  and  $\mu \rightarrow e\gamma$ . The parameters used are  $\tan \beta = 50$ ,  $p + n = 2$ ,  $n = -1$ ,  $r = -1$ ,  $a_{13} = 0$ , where the parameters refer to Eqs.37,38. As before, the remaining parameters  $A, a_{ij}$  are allowed to vary over the range 0.7–1.3 (and again typically good fits are obtained for values in the smaller range 0.9–1.1). The LSD prediction for  $\text{BR}(\mu \rightarrow e\gamma)$  in Figure 5(b) is comparable to that for the HSD model in Figure 2(b).

---

<sup>4</sup>In the finite 13 Yukawa case  $\theta_{13}$  is given by a more complicated formula [8]. However, the experimental limit on  $\text{BR}(\mu \rightarrow e\gamma)$  is a strong constraint in this case.

This is expected since the coefficient  $C_{21}$  for the LSD model in Eq.40 with  $p + n = 2$  is of similar magnitude to the coefficient  $C_{21}$  for the HSD model in Eq.28 with  $n = 2$ . The new feature in the LSD model is that the magnitude of  $\text{BR}(\tau \rightarrow \mu\gamma)$  in Figure 5(a) is now much smaller, and in fact is similar to the magnitude of  $\text{BR}(\mu \rightarrow e\gamma)$  in Figure 5(b), as predicted by Eq.41. However, if we had allowed  $X' < M_U$  then a larger, but still suppressed, prediction for  $\tau \rightarrow \mu\gamma$  following from Eq.42 would have been found. In any case the practical conclusion is the same: in the foreseeable future  $\tau \rightarrow \mu\gamma$  is experimentally unobservable for the LSD case. However  $\mu \rightarrow e\gamma$  may be observable and is determined by the choice of  $p + n$ , which we have taken to be  $p + n = 2$ . Figures 5(c),(d) show the accuracy of the LLA for the LSD class of models. As before the accuracy improves for larger SUSY masses but the error doubles in the evaluation of the branching ratio.

Note that in the case of the LSD class of models the branching ratio for  $\mu \rightarrow e\gamma$  can easily be enhanced by taking smaller  $p + n$  or suppressed by taking larger  $p + n$ , as is clear from Eq.40. Thus, a measurement of this branching ratio gives a measurement of the subleading Yukawa couplings of the second column, as in the HSD case. However, unlike the HSD case, the LSD case is not sensitive to the 13 slepton effect and the 13 Yukawa effect in Figures 3(b),(c). The effects beyond the leading mass insertion, due to a double slepton mass insertion, and effects coming from the Yukawa coupling parametrised by  $a_{31}$ , are both negligible for the LSD case. The reason that these effects were important for the HSD case was due to the large, order unity, Yukawa coupling in the 23 position. In the LSD case there are no large Yukawa couplings apart from that in the 33 position, and hence such effects are not so important in this case. This means that in the LSD case, the measurement of  $\text{BR}(\mu \rightarrow e\gamma)$  is more reliably related to a measurement of the Yukawa couplings parametrised by  $p + n$ .

## 4 Summary

This paper has focused on models which satisfy the sequential dominance condition. We have considered separately two broad classes of models, HSD and LSD, in which the dominant right-handed neutrino is the heaviest or lightest one. Although specific examples of models exist in the literature which satisfy either the HSD [21] or LSD [22] conditions, we emphasise that the sequential dominance condition is simply equivalent to assuming that a neutrino mass hierarchy is generated via the see-saw mechanism without fine-tuning in the leptonic sector, in the presence of large atmospheric and solar mixing angles. Therefore our results in fact apply to a very large class of models, although some of our specific results apply only in certain specific regions of parameter space.

We have presented approximate analytic results for neutrino masses and mixing angles, and for off-diagonal slepton masses in the leading log approximation in each case, using a new parametrisation of the matrices at the high energy scale. The parametrisation is very useful in relating the neutrino and LFV observables and in interpreting the data in terms of model parameters.

The numerical results, extracted from the best fits of the global top-down analysis, demonstrate the validity (limited, at times) of the leading log and leading mass insertion approximations used in the literature. We find that the magnitude of  $\text{BR}(\tau \rightarrow \mu\gamma)$  provides the main discriminator between the different classes of sequential dominance, with a large rate not far below current limits predicted by HSD, and a much smaller rate predicted by LSD. The observation of  $\text{BR}(\mu \rightarrow e\gamma)$ , on the other hand, may determine the order of the sub-dominant neutrino Yukawa couplings in the flavour basis in both the HSD and LSD cases. However, due to the large 23 Yukawa coupling, the results for HSD may be quite different from the leading log and leading mass insertion approximation predictions, making the interpretation of

$\text{BR}(\mu \rightarrow e\gamma)$  in terms of underlying Yukawa couplings more difficult, but still possible in principle. We have also shown that  $\text{BR}(\mu \rightarrow e\gamma)$  is independent of  $\theta_{13}$ , but measurement of this angle may determine a ratio of sub-dominant Yukawa couplings.

Ultimately one wants to use the observed neutrino data and constraints (or, if we are lucky, positive results) from the measurements of the  $\text{BR}(\tau \rightarrow \mu\gamma)$  and  $\text{BR}(\mu \rightarrow e\gamma)$  and other LFV processes to construct models and discriminate among them. To this end our study will serve as a framework for such top-down probes, and should help to establish: (i) if a sequential dominance mechanism is at work in the neutrino sector; (ii) if so then what type of dominance (HSD or LSD) is relevant; (iii) and then (subject to the exceptions discussed in section 3) the magnitude of the sub-leading neutrino Yukawa couplings in the flavour basis.

We emphasise how, within the framework of sequential dominance,  $\text{BR}(\tau \rightarrow \mu\gamma)$  and  $\text{BR}(\mu \rightarrow e\gamma)$  have a direct interpretation in terms of the underlying Yukawa couplings. It is worthwhile reiterating, however, that if there are additional sources of flavour violation, as generically expected in string theory [28], then these effects will need to be disentangled from the effects due to the RG running of the see-saw mechanism in the CMSSM discussed here. Also for simplicity we have neglected the effects of phases in a first global analysis of the CMSSM with a natural neutrino mass hierarchy, although our results demonstrate that the sign of Yukawa couplings can play an important part in determining the mixing angles.

## Acknowledgements

S.F.K. would like to thank A.Ibarra for useful comments. T.B. and S.F.K. thank PPARC and CERN for support for this work.

## References

- [1] Talks at XXth International Conference on Neutrino Physics and Astrophysics, Munich, May 25-30, 2002, <http://neutrino2002.ph.tum.de/>
- [2] M. Gell-Mann, P. Ramond and R. Slansky in Sanibel Talk, CALT-68-709, Feb 1979, and in *Supergravity* (North Holland, Amsterdam 1979); T. Yanagida in *Proc. of the Workshop on Unified Theory and Baryon Number of the Universe*, KEK, Japan, 1979.
- [3] R. N. Mohapatra and G. Senjanovic, Phys. Rev. Lett. **44** (1980) 912.
- [4] S. F. King, Phys. Lett. B **439** (1998) 350 [arXiv:hep-ph/9806440]; S. F. King, Nucl. Phys. B **562** (1999) 57 [arXiv:hep-ph/9904210].
- [5] R. Barbieri, P. Creminelli and A. Romanino, Nucl. Phys. B **559** (1999) 17 [arXiv:hep-ph/9903460].
- [6] G. Altarelli, F. Feruglio and I. Masina, Phys. Lett. B **472** (2000) 382 [arXiv:hep-ph/9907532].
- [7] S. F. King, Nucl. Phys. B **576** (2000) 85 [arXiv:hep-ph/9912492];
- [8] S. F. King, arXiv:hep-ph/0211228; S. F. King, JHEP **0209** (2002) 0411 [arXiv:hep-ph/0204360].
- [9] F. Borzumati and A. Masiero, Phys. Rev. Lett. **57** (1986) 961.
- [10] F. Gabbiani, E. Gabrielli, A. Masiero and L. Silvestrini, Nucl. Phys. B **477** (1996) 321 [arXiv:hep-ph/9604387].
- [11] J. Hisano, T. Moroi, K. Tobe and M. Yamaguchi, Phys. Rev. D **53** (1996) 2442 [arXiv:hep-ph/9510309].

- [12] S. F. King and M. Oliveira, Phys. Rev. D **60** (1999) 035003 [arXiv:hep-ph/9804283].
- [13] S. Ahmed *et al.* [CLEO Collaboration], Phys. Rev. D **61** (2000) 071101 [arXiv:hep-ex/9910060].
- [14] M. L. Brooks *et al.* [MEGA Collaboration], Phys. Rev. Lett. **83** (1999) 1521 [arXiv:hep-ex/9905013].
- [15] M. Roney [BABAR Collaboration], “Search for  $\tau \rightarrow \mu\gamma$  at BABAR”, talk at ICHEP2002, Amsterdam, July 2002.
- [16] Collaboration for the  $\mu \rightarrow e\gamma$  Experiment at PSI, “The  $\mu \rightarrow e\gamma$  Experiment - Goals and Status”, July 2002, available at <http://meg.web.psi.ch/docs/progress/jun2002/report.ps>
- [17] S. Davidson and A. Ibarra, JHEP **0109** (2001) 013; J. Hisano and D. Nomura, Phys. Rev. D **59** (1999) 116005; J. Hisano, arXiv:hep-ph/0204100; J. A. Casas and A. Ibarra, Nucl. Phys. B **618** (2001) 171; W. Buchmüller, D. Delepine and F. Vissani, Phys. Lett. B **459** (1999) 171; M. E. Gomez, G. K. Leontaris, S. Lola and J. D. Vergados, Phys. Rev. D **59** (1999) 116009; J. R. Ellis, M. E. Gomez, G. K. Leontaris, S. Lola and D. V. Nanopoulos, Eur. Phys. J. C **14** (2000) 319; W. Buchmüller, D. Delepine and L. T. Handoko, Nucl. Phys. B **576** (2000) 445; D. Carvalho, J. Ellis, M. Gomez and S. Lola, Phys. Lett. B **515** (2001) 323; F. Deppisch, H. Pas, A. Redelbach, R. Ruckl and Y. Shimizu, arXiv:hep-ph/0206122; J. Sato and K. Tobe, Phys. Rev. D **63** (2001) 116010; J. Hisano and K. Tobe, Phys. Lett. B **510** (2001) 197; J. R. Ellis, J. Hisano, M. Raidal and Y. Shimizu, Phys. Lett. B **528** (2002) 86, arXiv:hep-ph/0111324; J. R. Ellis, J. Hisano, S. Lola and M. Raidal, Nucl. Phys. B **621** (2002) 208, arXiv:hep-ph/0109125; J. Hisano, T. Moroi, K. Tobe and M. Yamaguchi, Phys. Lett. B **391**

(1997) 341; [Erratum - *ibid.* **397**, 357 (1997)]; J. Hisano, D. Nomura, Y. Okada, Y. Shimizu and M. Tanaka, Phys. Rev. D **58** (1998) 116010; J. Hisano, D. Nomura and T. Yanagida, Phys. Lett. B **437** (1998) 351.

[18] T. Blažek and S. F. King, Phys. Lett. B **518** (2001) 109 [arXiv:hep-ph/0105005].

[19] S. Lavignac, I. Masina and C. A. Savoy, Phys. Lett. B **520** (2001) 269 [arXiv:hep-ph/0106245]; S. Lavignac, I. Masina and C. A. Savoy, Nucl. Phys. B **633** (2002) 139 [arXiv:hep-ph/0202086].

[20] G. Altarelli and F. Feruglio, arXiv:hep-ph/0206077;

[21] S. F. King and M. Oliveira, Phys. Rev. D **63** (2001) 095004 [arXiv:hep-ph/0009287];

[22] S. F. King and G. G. Ross, Phys. Lett. B **520** (2001) 243 [arXiv:hep-ph/0108112];

[23] T. Blažek, M. Carena, S. Raby and C.E.M. Wagner, Phys. Rev. D **56**, 6919 (1997) [arXiv:hep-ph/9611217]; T. Blažek and S. Raby, Phys. Rev. D **59** (1999) 095002 [arXiv:hep-ph/9712257].

[24] T. Blažek and S. F. King, in preparation.

[25] G.W. Bennett, et al., Muon g-2 Collaboration, Phys. Rev. Lett. **89** (2002) 101804; Erratum-*ibid.* **89** (2002) 129903 [arXiv:hep-ex/0208001].

[26] K. Hagiwara, A. D. Martin, Daisuke Nomura and T. Teubner, [arXiv:hep-ph/0209187].

[27] H. Fritzsch and Z. z. Xing, Prog. Part. Nucl. Phys. **45** (2000) 1 [arXiv:hep-ph/9912358].

[28] G.G.Ross and O.Vives, hep-ph/0211279.

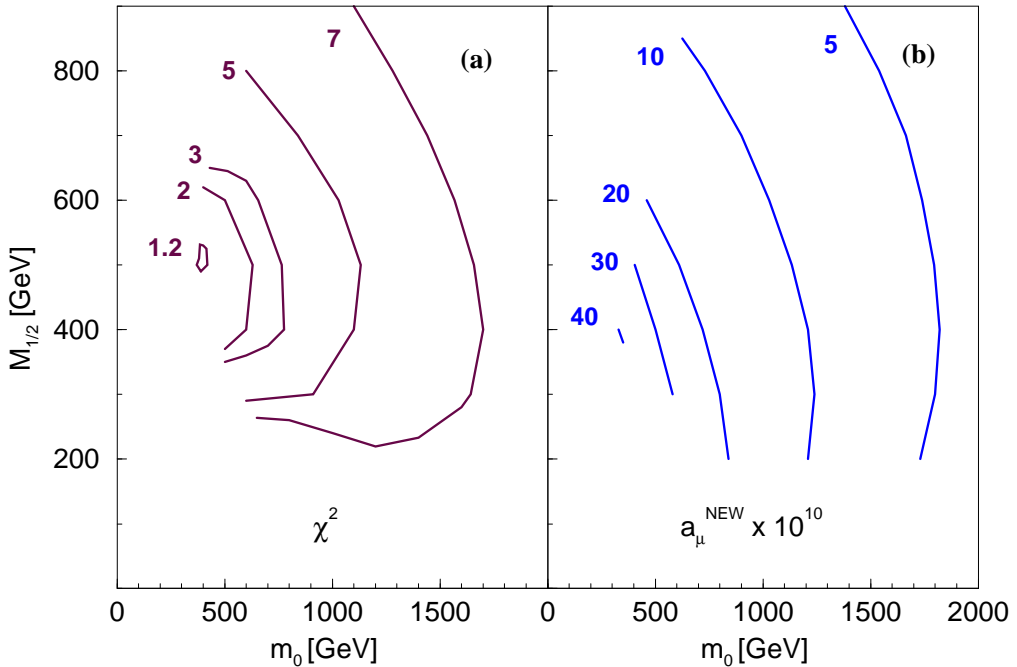


Figure 1: Results for the global analysis of HSD. We use the baseline parameters  $\tan \beta = 50$ ,  $n = 2$ ,  $r = -1$ ,  $a_{13} = 0$ . Panel (a) shows the  $\chi^2$  of the fit which is minimised for  $m_0 \sim M_{1/2} \sim 500$  GeV. Panel (b) shows the SUSY contribution to the anomalous magnetic moment of the muon.

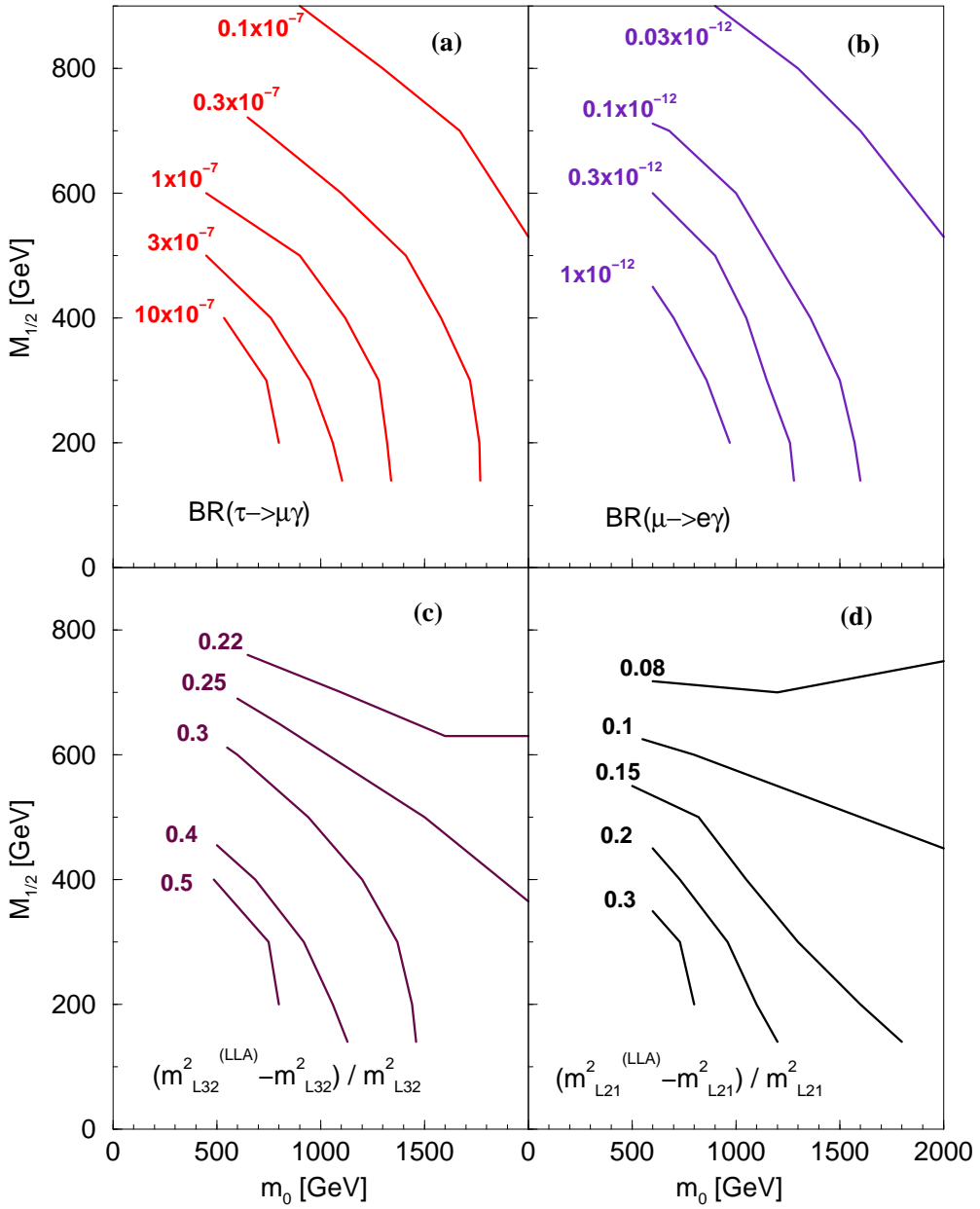


Figure 2: The upper panels show the predictions for the branching fraction for (a)  $\tau \rightarrow \mu\gamma$  and (b)  $\mu \rightarrow e\gamma$  for HSD using the same baseline parameters as in Figure 1. The lower panels (c), (d) show the fractional error  $\Delta_{ij}$ , defined in the text, that would be made in calculating the off-diagonal slepton masses if the leading log approximation had been used instead of the exact calculation.

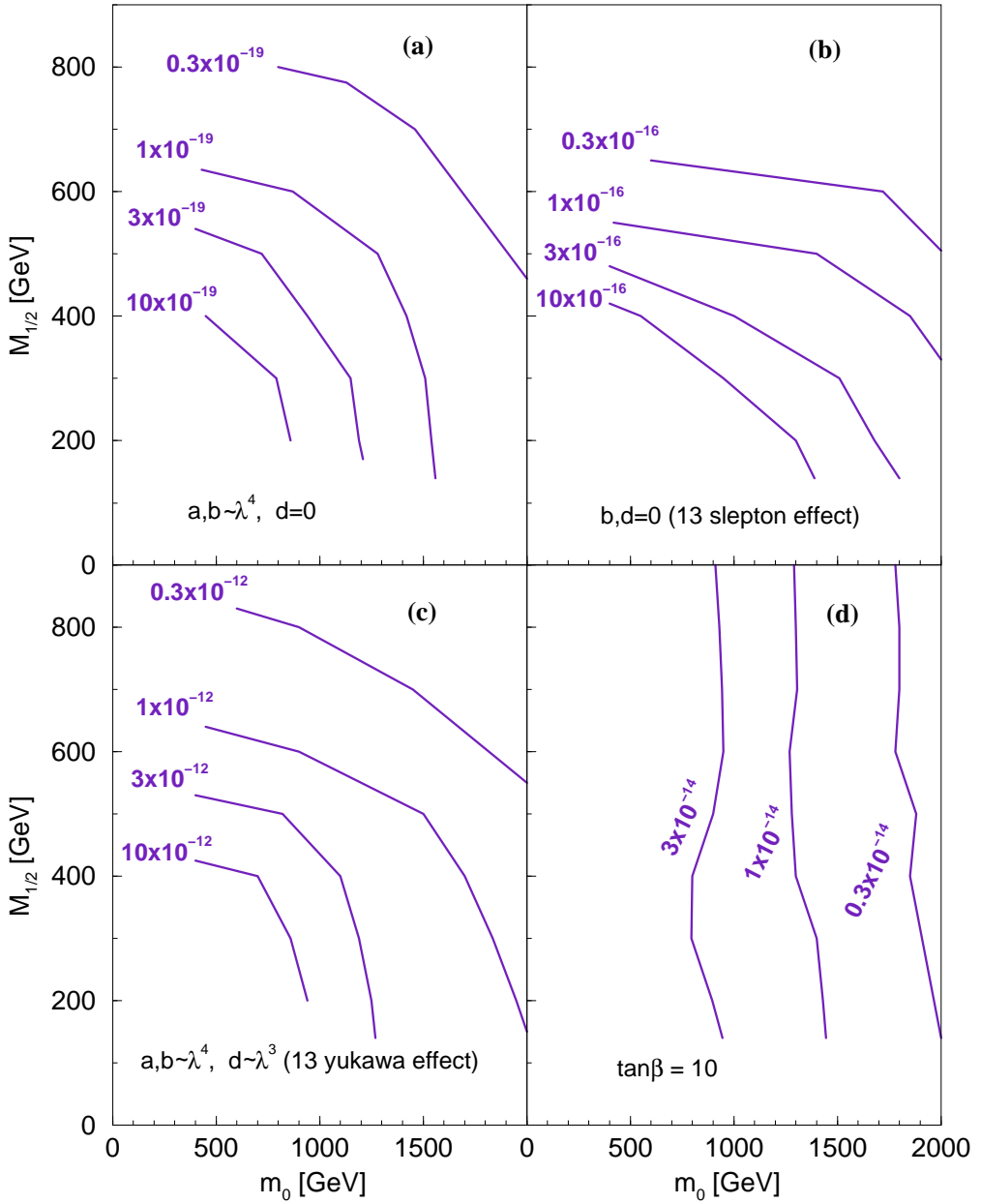


Figure 3: Predictions for  $\text{BR}(\mu \rightarrow e\gamma)$  in HSD for alternative choices of parameters in this class of models. In panel (a), we choose  $\tan\beta = 50$ ,  $n = 4$ ,  $r = -1$ ,  $a_{13} = 0$ . In panel (b) we choose  $\tan\beta = 50$ ,  $n = 2$ ,  $r = 0$ ,  $a_{13} = 0$ ,  $a_{22} = 0$ . In panel (c) we choose  $\tan\beta = 50$ ,  $n = 4$ ,  $r = -1$ ,  $m = 3$ . In panel (d) we choose  $\tan\beta = 10$ ,  $n = 2$ ,  $r = -1$ ,  $a_{13} = 0$ .

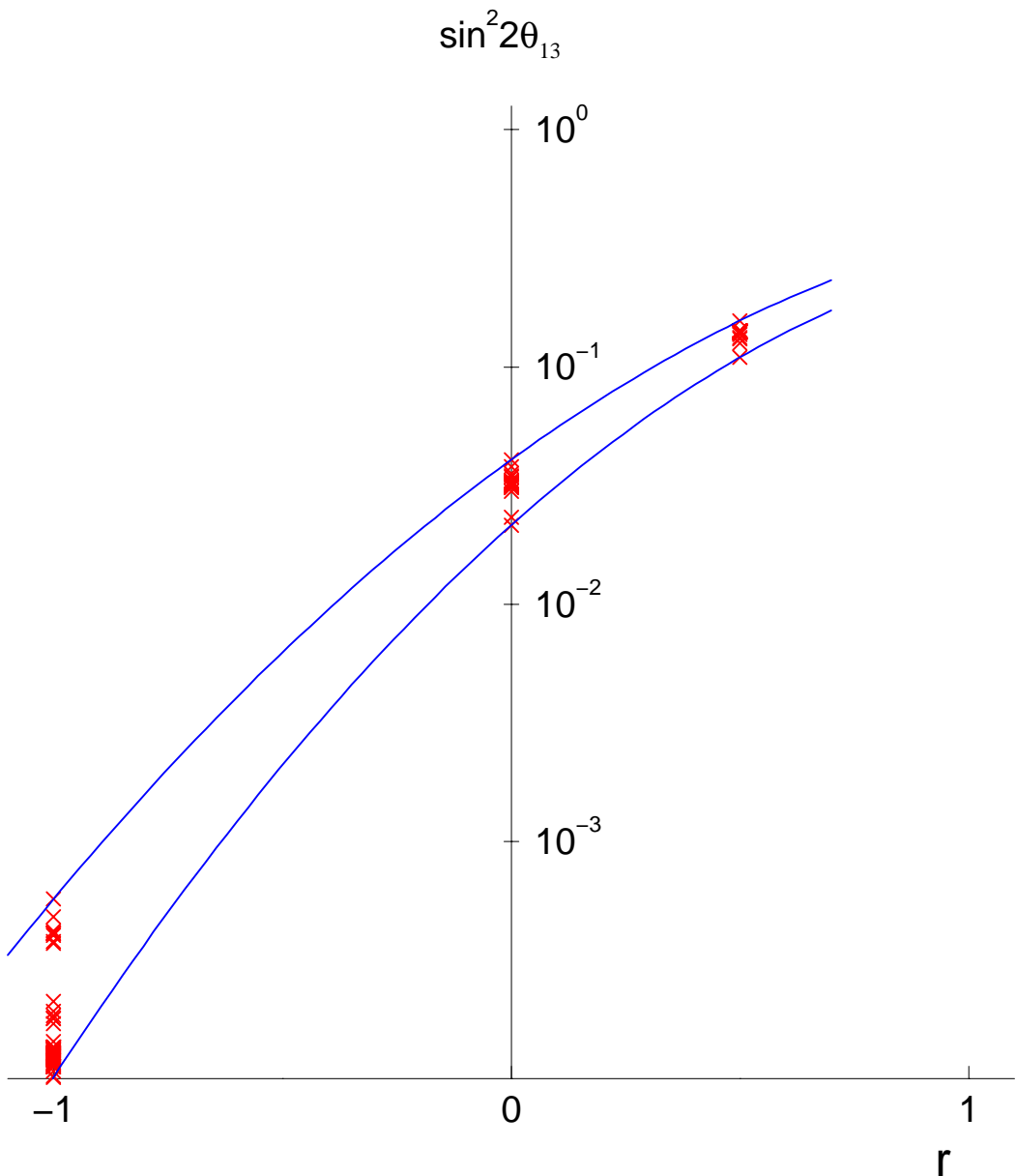


Figure 4: The prediction of  $\sin^2 2\theta_{13}$  as a function of the ratio of subdominant Yukawa couplings  $r = a_{32}/a_{22}$  for the HSD class of models. The remaining parameters are as in Figure 1.

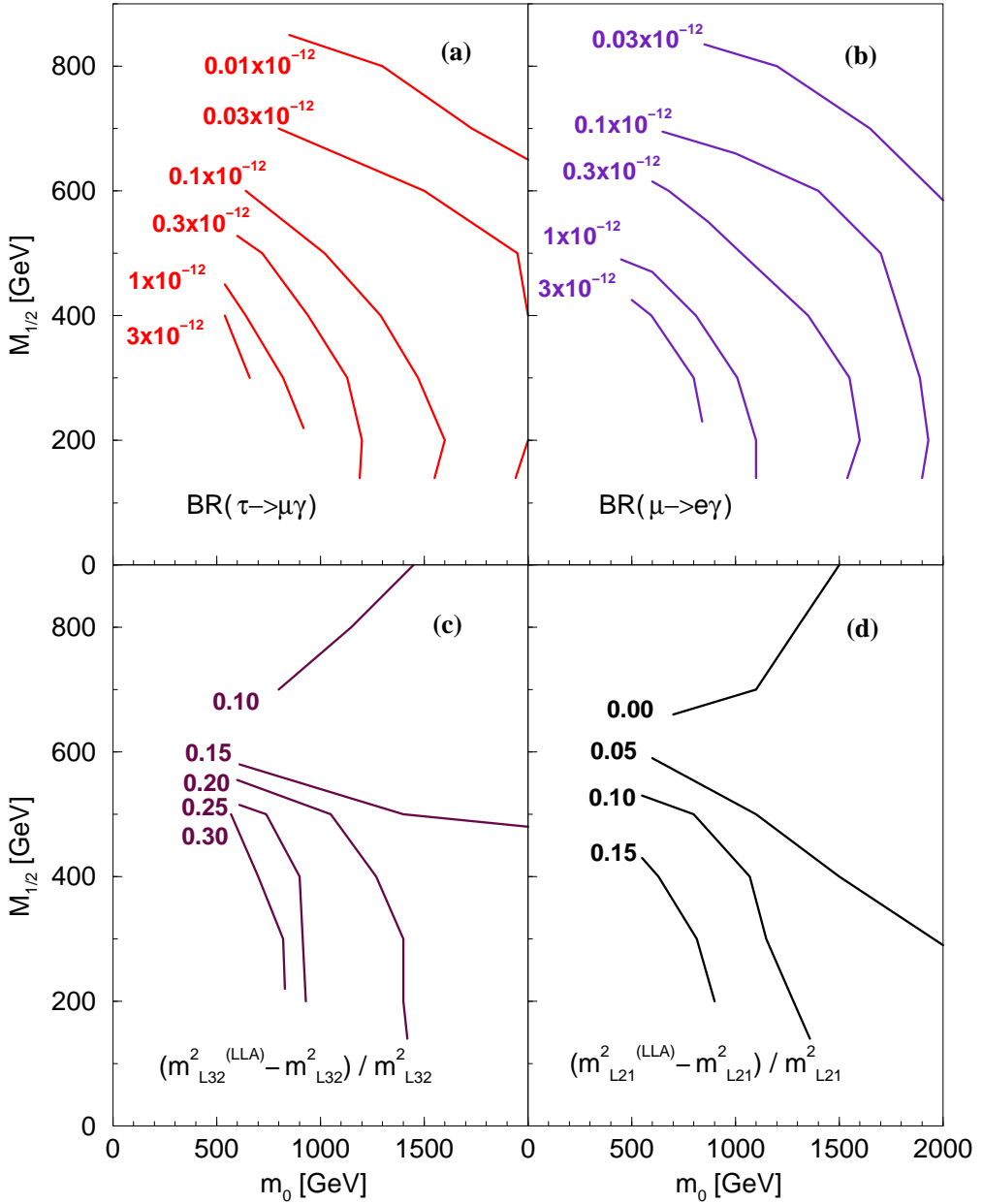


Figure 5: The upper panels show the predictions for the branching fraction for (a)  $\tau \rightarrow \mu\gamma$  and (b)  $\mu \rightarrow e\gamma$  for the LSD class of models. The parameters used are  $\tan \beta = 50$ ,  $p + n = 2$ ,  $n = -1$ ,  $r = -1$ ,  $a_{13} = 0$ . The lower panels (c), (d) show the fractional error  $\Delta_{ij}$ , defined in the text, that would be made in calculating the off-diagonal slepton masses if the leading log approximation had been used instead of the exact calculation.